International Journal of Pharmaceutics 423 (2012) 496–508

Contents lists available at SciVerse ScienceDirect

International Journal of Pharmaceutics

journal homepage: www.elsevier.com/locate/ijpharm

Pharmaceutical nanotechnology

Preparation and characterization of hydroxypropyl methyl cellulose films containing stable BCS Class II drug nanoparticles for pharmaceutical applications

Lucas Sievens-Figueroa[a], Anagha Bhakay[a], Jackeline I. Jerez-Rozo[b], Natasha Pandya[a], Rodolfo J. Romañach[b], Bozena Michniak-Kohn[d], Zafar Iqbal[c], Ecevit Bilgili[a], Rajesh N. Davé[a,*]

[a] Department of Chemical, Biochemical, and Pharmaceutical Engineering, New Jersey Institute of Technology, United States
[b] Department of Chemistry, University of Puerto Rico, Mayagüez Campus, United States
[c] Department of Chemistry and Environmental Science, New Jersey Institute of Technology, United States
[d] Department of Pharmaceutics, Ernest Mario School of Pharmacy, Rutgers-The State University of New Jersey, United States

ARTICLE INFO

Article history:
Received 7 October 2011
Received in revised form
29 November 2011
Accepted 1 December 2011
Available online 9 December 2011

Keywords:
Nanosuspensions
Media milling
BCS Class II
Pharmaceutical films
Hydroxylpropyl methyl cellulose

ABSTRACT

The design and feasibility of a simple process of incorporating stable nanoparticles into edible polymer films is demonstrated with the goal of enhancing the dissolution rate of poorly water soluble drugs. Nanosuspensions produced from wet stirred media milling (WSMM) were transformed into polymer films containing drug nanoparticles by mixing with a low molecular weight hydroxylpropyl methyl cellulose (HPMC E15LV) solution containing glycerin followed by film casting and drying. Three different BCS Class II drugs, naproxen (NPX), fenofibrate (FNB) and griseofulvin (GF) were studied. The influence of the drug molecule on the film properties was also investigated. It was shown that film processing methodology employed has no effect on the drug crystallinity according to X-ray diffraction (XRD) and Raman spectroscopy. Differences in aggregation behavior of APIs in films were observed through SEM and NIR chemical imaging analysis. NPX exhibited the strongest aggregation compared to the other drugs. The aggregation had a direct effect on drug content uniformity in the film. Mechanical properties of the film were also affected depending on the drug–polymer interaction. Due to strong hydrogen bonding with the polymer, NPX exhibited an increase in Young's Modulus (YM) of approximately 200%, among other mechanical properties, compared to GF films. A synergistic effect between surfactant/polymer and drug/polymer interactions in the FNB film resulted in an increase of more than 600% in YM compared to the GF film. The enhancement in drug dissolution rate of films due to the large surface area and smaller drug particle size was also demonstrated.

1. Introduction

The solubility of drug molecules is an important factor to take into account during the development and design of new drug products. According to the Biopharmaceutical Classification System (BCS), Class II drugs are characterized by their poor solubility and high permeation in the human body (Amidon et al., 1995). The hydrophobicity becomes essential for their transport properties through the cell membrane and their pharmacological action to be exerted in the desired tissue. Since these compounds have low solubility, limited bioavailability is observed (Krishnaiah, 2010; Kesisoglou et al., 2007). In order to overcome this limitation, a commonly used approach involves particle size reduction (Merisko-Liversidge and Liversidge, 2011; Liversidge and Cundy, 1995; Muller, 2011; Keck and Muller, 2006; Pu et al., 2009; Timpe, 2010; Gao et al., 2008; Pathak et al., 2005; Panagiotou and Fisher, 2008). By reducing the particle size it is expected that the dissolution rate will be increased as described mathematically by the Noyes–Whitney equation (Noyes and Whitney, 1897).

Among the methods used for particle size reduction the use of wet stirred media milling (WSMM) has received much attention because of the effectiveness in producing microparticles and nanoparticles (Bhakay et al., 2011; Merisko-Liversidge and Liversidge, 2011; Merisko-Liversidge et al., 2003). WSMM has been extensively used to formulate nanoparticles of drugs that are poorly soluble into nanosuspensions that can be used orally or can be used in ocular delivery, intravenous administration and dermal applications (Mauludin et al., 2009; Shegokar and Müller, 2010; Rabinow et al., 2007; Petersen, 2006; Piao et al., 2008; Hernandez-Trejo et al., 2005). In order to take advantage of the bioavailability enhancement it is necessary for the particle size to be preserved after administration. In general, this becomes problematic since particles tend to aggregate due to their large surface area and need to be stabilized (Bilgili et al., 2006; Mende et al., 2003; Peukert et al.,

* Corresponding author. Tel.: +1 973 596 5860; fax: +1 973 642 7088.
E-mail address: dave@adm.njit.edu (R.N. Davé).

0378-5173/$ – see front matter © 2011 Elsevier B.V. All rights reserved.
doi:10.1016/j.ijpharm.2011.12.001

2005). Without a means to functionalize the surface, nanoparticles will tend to aggregate to a less energetic state. Polymers and surfactants are used as stabilizers to minimize particle aggregation (Van Eerdenbrugh et al., 2009). The stabilizers adsorb on the surfaces of the drug particles and provide an ionic or steric barrier (Merisko-Liversidge et al., 2003; Ploehn and Russel, 1990).

A significant amount of the work in the literature has focused on process improvement, characterization and stability of nanosuspensions (Choi et al., 2005; Verma et al., 2011; Van Eerdenbrugh et al., 2009). Stability of nanosuspensions could become challenging and therefore solid dosage forms are preferred (Bhakay et al., under review; Van Eerdenbrugh et al., 2008c). Solid dosage forms are also considered more attractive due to their convenience and consumer preference aspects. However, in order to prepare them, nanosuspensions have to be dried, which would likely lead to agglomeration of the nanoparticles, poor re-dispersion and poor recovery of nanoparticles (Heng et al., 2010; Bhakay et al., under review; Van Eerdenbrugh et al., 2008a,b; Lee and Cheng, 2006; Lee, 2003; Kim and Lee, 2010; Choi et al., 2008; Hu et al., 2011; Cheow et al., 2011). Most of the transformation of nanosuspensions into solid products presented in literature use well known unit-operations such as freeze-drying, spray-drying, pelletization and granulation (Van Eerdenbrugh et al., 2008a; Müller et al., 2006). Further processing of those powders in capsule filling or compression into tablets can also be performed (Vergote et al., 2001; Heng et al., 2010). In previous work, Desieno and Stetsko (1996) described the use of carrier particles, such as sugar or microcrystalline cellulose, coated with films containing nanoparticles utilizing WSMM. They showed re-dispersion and size preservation of the nanoparticles from the coated carrier utilizing stabilizers. Wax based pellets loaded with nanocrystalline ketoprofen have also been studied and the enhancement in dissolution compared to the microcrystalline form shown (Vergote et al., 2001). While the transformation of nanoparticles from WSMM to common solid dosage forms has been presented, the integration of WSSM into polymer films remains to be well studied. Polymer films can be an effective carrier of nanoparticles to mitigate the aforementioned problems and enhance dissolution of poorly water-soluble drugs, hence integration of WSSM into polymer films is warranted.

Polymer films (PF) have great potential over other dosage forms for delivery of poorly soluble drugs since they provide distinct advantages over other oral formulations including larger surface area which leads to rapid disintegration and dissolution in the oral cavity and increased bioavailability (Dixit and Puthli, 2009). This allows for a more rapid and controlled wetting in the oral or buccal environment. PF are easy to swallow and are a convenient dosage form and this has also led to improved acceptability and compliance among the geriatric and pediatric patients. PF also exhibit manufacturing advantages including continuous manufacturing capabilities that enable full product characterization when incorporated with in-line monitoring using Process Analytical Technologies (PAT) (Dixit and Puthli, 2009). Even though the interest in pharmaceutical films has increased based on publications and patents (Boateng et al., 2010; Matthews et al., 2008; Garsuch and Breitkreutz, 2010; Mendoza-Romeroa et al., 2009; Li and Gu, 2007; El-Setouhy and Abd El-Malak, 2010; Perumal et al., 2008; Bess et al., 2010; Yang et al., 2010, 2011), more research is needed in order to overcome potential limitations and increase the general patient acceptance.

Research in this field has focused on the incorporation of water-soluble drugs into film formulations (Jug et al., 2009; Nishimura et al., 2009; Schmidt and Bodmeier, 1999; Shimoda and Taniguchi, 2009). While water soluble drugs exist in the dissolved state or as solid solution, the water insoluble drugs have to be homogenously distributed in a film formulation in order to have an acceptable drug content uniformity. In recent patents (Yang et al., 2010, 2011) the process for making films with uniform distribution of components is described. The incorporation of poorly soluble particles into films or the issues involved when using microparticles or nanoparticles were not specifically addressed in these patents. Interactions between the drug molecule and polymer could also produce differences in the film properties (Nair et al., 2001). In this work we use a simple process for the preparation of films containing dispersed nanoparticles as the final dosage form for drug delivery applications. WSMM is used to produce stable BCS Class II drug nanosuspensions that are then transformed into polymeric films containing stable drug nanoparticles. The objective of this work was to demonstrate the feasibility and set the groundwork for the integration of WSMM with pharmaceutical polymer films formulations. A range of BCS Class II drugs that includes griseofulvin, fenofibrate and naproxen were used. The particle size distribution of the nanosuspensions and re-dispersion of the drug particles from films were investigated by utilizing laser diffraction. Distribution of drug particles in film was studied by NIR Chemical Imaging (Jérez Rozo et al., 2011). The influence of the drug molecule on the film mechanical properties was also studied. The morphology of the particles from suspensions and the structure of the films were observed by using Scanning Electron Microscopy (SEM). The crystallinity of drug particles before milling and in films was studied by X-ray diffraction (XRD) and Raman spectroscopy. The drug content for film containing nanoparticles with different thicknesses was studied, and the dissolution behavior was compared to different solid dosage forms and films containing microparticles.

Table 1
Physicochemical properties of the drugs.

Drug	Solubility (mg/l)	Molecular weight	Melting point (°C)	log *P*	Particle size (μm)		
					D_{10}	D_{50}	D_{90}
FNB	0.50	360.8	80.5	4.4	4.6	13.2	34.2
GF	8.99	352.8	220.0	3.5	5.2	11.8	23.6
NPX	17	230.26	153	3.0	3.2	11.5	26.7

2. Materials and methods

2.1. Materials

The drug molecules utilized were griseofulvin (GF; Sigma–Aldrich, Saint Louis, MO), naproxen (NPX; Medisia, NY, USA), and fenofibrate (FNB; Ja Radhe Sales, Ahmedabad, India). Chemical structures of the drug molecules are shown in Fig. 1. Sodium dodecyl sulfate (SDS) (Sigma–Aldrich, Saint Louis, MO) and low molecular weight hydroxypropyl methyl cellulose (HPMC; Methocel E15LV) (Dow Chemical) were used as a stabilizer. HPMC (Methocel E15LV) was also used as a film former. Glycerin (Sigma) was used as a plasticizer. All these materials were used without further processing.

2.2. Methods

2.2.1. Preparation of drug nanosuspensions

FNB, GF and NPX were chosen as the model BCS Class II drugs. The physicochemical properties of these drugs are given in Table 1. The initial particle sizes of all the drugs were slightly different as seen in Table 1. The formulation of the suspensions and the milling time for each of the drugs differed based on the optimization studies performed in our group. The formulation of the suspensions was optimized for all the drugs in a separate study, which was guided by the work in Bhakay et al. (2011, under review) and will be presented in a forthcoming paper. The HPMC concentration was kept constant at 2.5% (w/w) (wrt water) for all the drugs. The SDS concentration was 0.5% (w/w) (wrt water) for GF and NPX suspensions and was reduced to 0.075% (w/w) (wrt water) for FNB suspension. A low

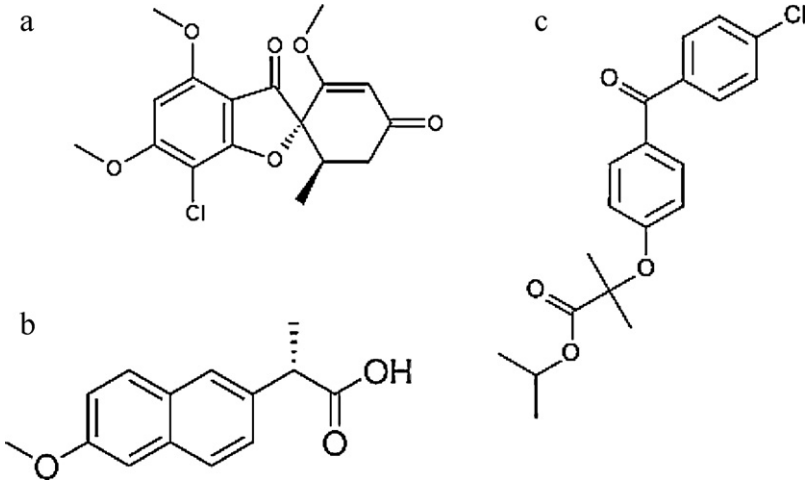

Fig. 1. Chemical structures of BCS Class II drug molecules used in this study: (a) GF, (b) NPX and (c) FNB.

SDS concentration (0.5%) was selected for FNB suspensions in the presence of 25% HPMC because a physical stability issue at high SDS concentration (5%) was observed. Particle size increased notably (90% passing size increased from 230 nm to 1025 nm) during 7-day storage even in refrigerated conditions (8 °C) via agglomeration and Ostwald ripening mechanisms.

The procedure of preparation of all the suspensions was identical. HPMC was dissolved in 200 g de-ionized water using a shear mixer (Fisher Scientific Laboratory stirrer, Catalog no. 14-503, Pittsburgh, PA, USA) running at a fixed speed of 300 rpm for 30 min to make a 2.5% (w/w) HPMC solution. SDS was then dissolved in the HPMC solution and stirred for 15 min. 10% (w/w) (wrt water) drug was then dispersed into the stabilizer solution with the shear mixer running for 30 min. The NPX suspensions had a pH of 5.3. A sample of the drug suspension was taken at the end of mixing and was reported as the initial particle size of the drug in Table 1.

Drug suspensions prepared via mixing, as mentioned above, were subsequently milled in a Netzsch wet media mill (Microcer, Fine particle technology LLC, Exton, PA, USA). Zirconia beads with a nominal size of 400 μm were used as the milling media and a 200 μm screen was used to retain the beads in the milling chamber. Zirconia beads with a 50 ml bulk volume were loaded to the milling chamber (80 ml capacity). The drug suspension was loaded in the holding tank and pumped through the milling chamber at a fixed speed of 126 ml/min using a peristaltic pump. The FNB, GF and NPX suspensions were milled for 120, 60, and 90 min, respectively at a tip speed of about 10.5 m/s. Different milling time was used for the drugs to get the median particle size in the range of 150–250 nm at the end of milling. The temperature inside the mill was maintained at less than 32 °C with the help of a chiller (Advantage Engineering, Inc., Greenwood, IN, USA). The mill was run in the recirculation mode of operation. In this mode, the suspension circulates from the holding tank passing through the milling chamber, exits through the screen and returns back to the holding tank. High speed rotation of the rotor in the milling chamber induces turbulent motion in the suspension, and turbulent energy dissipates through frequent bead–bead collisions (Eskin et al., 2005), which cause extensive breakage of drug particles captured between the beads (Bilgili et al., 2004, 2006; Bhakay et al., 2011).

2.2.2. Particle size distribution

The particle size distribution of suspensions was measured by laser diffraction in Coulter LS13320 (Beckman Coulter, Miami, FL, USA) without the use of built-in sonication feature available in the instrument. A sample of the suspension was taken at the end of milling from the holding tank of the mill while the suspension was being stirred. The sample was dispersed in 15 ml of the stabilizer solution containing HPMC and SDS corresponding to the formulation that was being milled, by stirring with a pipette. The sample was added drop-wise until the polarization intensity differential scattering (PIDS) reached 40% for all the samples.

The same method was used to measure the particles size of nanoparticles re-dispersed from films. Circular films with an area of 0.71 cm^2 and an average thickness of 100 μm were put in approximately 15 ml of de-ionized water (concentration above the solubility for all drugs) for film disintegration. The sample particle size was measured after 10 min of magnetic stirring.

2.2.3. Preparation of films containing nanoparticles

Fig. 2 shows a schematic of the process used for film formation. A solution containing 10% HPMC (wrt to solution weight) (10 g) and 10% glycerin (wrt to solution weight) (10 g) was prepared by adding the glycerin to water (80 g) and heating to 80 °C. This composition was chosen based on preliminary work, taking into account the final suspension viscosity and film quality. The polymer was then added until well dispersed and the temperature was decreased to room temperature to dissolve the polymer completely. The components were mixed until a clear solution was obtained. The resulting solution was then let to rest until no bubbles were seen. The polymer solution (50 g) was then added to the nanosuspension produced from WSMM (50 g), and then mixed for 3 h using a dual-propeller mixer (McMaster, Catalog no. 3471K5, Los Angeles, CA, USA) attached to a motor (VWR OVERHEAD STIR VOS 16V120) and left to rest until no bubbles were observed. The final GF suspensions had 6.11% HPMC, 4.42% GF, 5.00% glycerin, and 0.22% SDS. NPX suspensions had the same weight % composition. On the other hand, the FNB suspensions had a lower SDS concentration (6.11% HPMC, 4.42% FNB, 5.00 glycerin, and 0.03% SDS). The final viscous suspension was then casted onto a stainless steel plate using a Doctor Blade (Elcometer, USA). The wet film thickness was varied from 600 μm to 1400 μm by changing the Doctor Blade aperture to study the impact of thickness on drug composition. The film was then dried overnight in an oven (Gallenkamp 300 Plus Series, UK) at 42 °C. The theoretical amount of drug in the resulting films accounted for 27% (w/w) of the film composition.

2.2.4. Preparation of films containing microparticles

A solution containing 8% HPMC (wrt to solution weight) (8 g) and 5.2% glycerin (wrt to solution weight) (5.2 g) was prepared by adding the glycerin to water (86.8 g) and heating to 80 °C. This

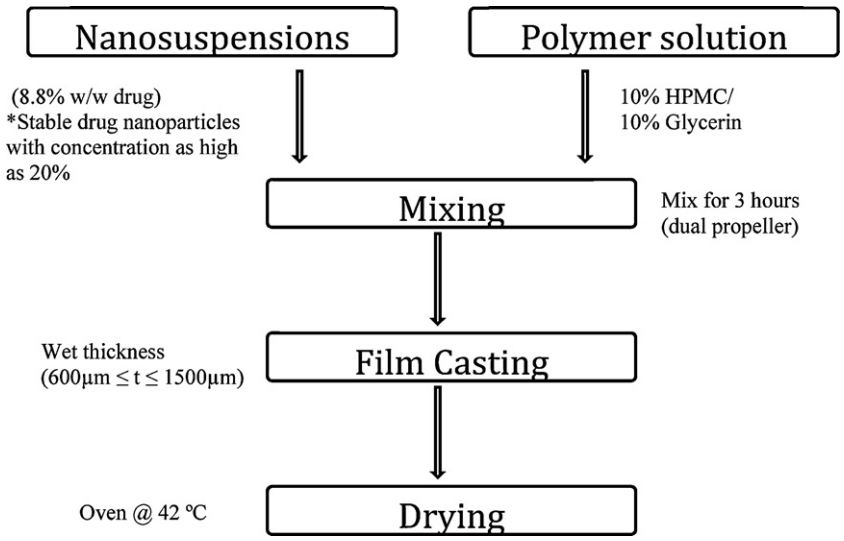

Fig. 2. Process schematic for the integration of WSMM nanosuspensions and films.

composition was chosen in order to obtain similar drug concentration as the film containing nanoparticles. The polymer was then added until well dispersed and the temperature was decreased to room temperature to dissolve the polymer completely. The components were mixed until a clear solution was obtained. The polymer solution (50 g) was then mixed with FNB (2.3 g) and SDS (0.015 g) followed by casting with a thickness of 1000 μm and drying using the same procedures mentioned above. The final GF suspensions had 6.53% HPMC, 4.40% FNB, 4.97% glycerin, and 0.03% SDS.

2.2.5. Film characterization

2.2.5.1. Film thickness. The thickness of the different films was measured using a digital micrometer (Mitutoyo, Japan) with an accuracy of 0.001 mm. Thickness was measured in 4 different locations of the film and the average thickness was used.

2.2.5.2. SEM. Field emission scanning electron microscope (FESEM) LEO1530VP GEMINI (Carl Zeiss, Inc., Peabody, MA, USA) was used to observe the morphology of particles produced from WSMM and the distribution of particles in films. A drop of the nanosuspension was placed on the silicon chip placed on top of carbon tape and left overnight to dry under vacuum. A small piece of the film was placed on the carbon tape for the analysis of the films. Samples were carbon coated using a sputter coater (Bal-Tec MED 020 HR) before analysis.

2.2.5.3. XRD. X-ray diffraction was performed to determine the crystallinity of unprocessed drug and drug incorporated in films. Diffraction patterns were acquired for analysis of amorphous/crystalline behavior of processed drugs from Philips X'Pert (Almelo, Netherlands).

2.2.5.4. NIR chemical imaging. Near infrared Hyperspectral images were acquired using the Malvern SyNIRgi NIR-CI System (Malvern, UK). The images were obtained in transflectance mode by placing the film over a white ceramic disk of a 28 mm diameter. The optical magnification used was 131 μm which provide images of an area of approximately 34 mm × 42 mm, respectively. The spectra were obtained with 1 scan in the spectral range of 1300–2300 nm. The data collected was analyzed using the ISys Version 5.0.0.14 software.

The logarithm, log10 (1/*R*), was first applied to the data cube to convert the spectra to absorbance units. Pixel correction was applied in order to remove areas of non-uniform illumination and to remove the effect of unresponsive pixels on the detector. The spectra were normalized using Standard Normal Variate (SNV) and a Savitzky–Golay second derivative (filter order 3, filter width 7) in order to eliminate variations in slope. The spectral range was restricted to 2000–2300 nm; as this spectral range provides the greatest differences between excipients and different drugs, and water does not absorb NIR radiation in this region (Chan and Kazarian, 2004). Pure component imaging data were collected from powder samples of the drugs and excipients and processed in the same manner. The pure component training spectra were used as predictors to build a partial least squares (PLS-DA) classification model. The intensity of each pixel in the resultant scores image is determined by the degree of membership (scaled from 0 to 1). The variation in pixel intensity reflects the variation in concentration across the sample.

2.2.5.5. Raman spectroscopy. An EZRaman LE Raman Analyzer system from Enwave Optronics (Irvine, CA) with an HRP 8 high throughput fiber probe coupled to a MicroView adapter with a 10× objective 10 μm spot size and a 250 mW 785 nm was used for measurements on the powder and film samples. Raman spectra collected corresponded to an average of 5 scans with 10 s acquisition time each.

2.2.5.6. Mechanical properties. Mechanical properties testing were conducted using a TA-XT Plus Texture Analyzer (Stable Microsystems, UK). The film was cut into 3.0 cm × 1.5 cm strips for the tensile test. Film thickness was measured at 4 different locations of the films and the average was used. The sample was attached to the tensile grips and the test was finished once the sample broke. A test speed of 1 mm/s was employed. Tensile strength (TS), elongation at break (*E*) and Young's modulus (YM) were computed to evaluate the tensile properties of the films (Radebaugh et al., 1988). TS was calculated by dividing the maximum force by the original cross-sectional area of the specimen and it was expressed in force per unit area (kPa). YM was calculated as the slope of the linear portion of the stress–strain curve and it was also expressed in force per unit area (kPa). *E* was calculated by dividing the extension at the moment of film rupture by the initial length of the specimen and multiplying by 100. The average and standard deviation for three samples were recorded.

A rupture test was also performed by using the compression mode and a film support rig with 5 mm stainless steel ball probe. A circular strip film with an area of 3.88 cm^2 was used. The film support rig was fitted to the heavy duty platform and positioned loosely on the machine base. The ball probe was connected to the load cell with a probe adaptor and the film support rig was aligned with the ball probe to ensure the probe can move centrally through the aperture without contacting the film support rig. The force needed to break the film was calculated. The average and standard deviation for three samples were also recorded.

2.2.5.7. Determination of drug content in films. The drug content in the films was determined using an Agilent 1100 series HPLC system consisting of a pump and a UV detector. Batches with different thicknesses were casted and 10 strip films from each batch were tested. Films were cut in circular samples with an area of 0.712 cm^2. Samples were then dissolved in 250 ml of 0.019 M SDS, 0.025 M SDS, and phosphate buffer solution (PBS, pH 7.2) for GF, FNB, and NPX, respectively. The concentration was then calculated using the average of the 10 strip films.

Griseofulvin method. UV detection at 295 nm was used with a Waters Spherisorb 10 μm CN analytical column (4.6 mm × 250 mm). The temperature was maintained at 25 °C. The mobile phase was a mixture of water and acetonitrile (50:50, v/v) with a flow rate of 1.0 ml/min. The samples were put into HPLC vials and 20 μl automatically injected into the HPLC system. The concentration was determined from a calibration curve.

Fenofibrate method. UV detection at 270 nm was used after separation with an Agilent Microsorb-MV 100-5 C18 analytical column (4.6 mm × 150 mm). The temperature was maintained at 25 °C. The mobile phase was a mixture of water and acetonitrile (30:70, v/v) with a flow rate of 1.0 ml/min. The samples were put into HPLC vials and 20 μl automatically injected into the HPLC system. The concentration was determined from a calibration curve.

Naproxen method. UV detection at 270 nm was used with an Agilent-Eclipse XDB-C18 analytical column (4.6 mm × 150 mm). The temperature was maintained at 25 °C. The mobile phase was a mixture of water and methanol (50:50, v/v) with a flow rate of 1.2 ml/min. The samples were put into HPLC vials and 20 μl automatically injected into the HPLC system. The concentration was determined from a calibration curve.

2.2.5.8. Dissolution. Dissolution experiments were performed using a flow-through cell dissolution apparatus (USP IV, Sotax, Switzerland) with cells of an internal diameter of 22.6 mm (Kakhi, 2009; Heng et al., 2008). Films were horizontally positioned in the cells with 6.5 g of glass beads (1 mm in diameter) filling up the conical part at the bottom of each cell. Glass microfiber filters (GF/D grade) were used in the filter-head in each experiment unless otherwise mentioned. The temperature was maintained at 37 ± 0.5 °C and a flow rate of 16 ml/min was used. During testing, the dissolution medium (900 ml) was circulated by pumping it through each cell. SDS solution (0.025 M) was used as dissolution mediums for FNB. FNB was chosen to perform dissolution studies because of the interest of improving the bioavailability of this drug (Hanafy et al., 2007; Stamm and Seth, 2001; Ryde et al., 2008). A Thermo Evolution UV spectrophotometer was used to automatically measure the FNB concentration using a previously made calibration curve. Six samples were used and the average drug release and standard deviation were plotted as a function of time. Films with an area of 0.71 cm^2 and an average thickness of 110 μm were used for the dissolution test.

Films containing FNB microparticles were also tested for dissolution. In order to confirm the enhancement of dissolution of films compared to other solid dosage forms, a sample containing FNB microparticles (with a median particle size in suspension of 11 μm) (41%, w/w), HPMC (57%, w/w), and SDS (2%, w/w) was mixed using a resonant acoustic mixer (LabRam, Resodyn, Montana, USA). The ratio HPMC/FNB (1.39) and FNB/SDS (20.5) was kept the same as present in the films. A total of 20 g were mixed for 10 min at 85 Gs. 200 mg of the physical mixture were tested for dissolution. The physical mixture was also transformed into a compact (200 mg) by using a Carver single punch compressing machine (model 3851-0, Indiana, USA). The sample was compressed using 22,200 N for 3 min of compression time with a 10 mm diameter punch. Films containing FNB microparticles were also used to compare dissolution of microparticles and nanoparticles incorporated in films. The same dissolution cell and procedure employed for films were also used for tablets and physical mixtures.

3. Results

3.1. Production and characterization of nanosuspensions

Stable nanosuspensions for each drug were produced by utilizing HPMC and SDS as stabilizers during WSMM. Long term stability of the suspensions and optimization of the stabilizers for long-term stability were are not considered in this work. Fig. 3 shows the cumulative particle size distribution for the three different nanosuspensions after wet media milling used in this work. GF, FNB and NPX suspensions exhibit a median particle size of 163 nm, 201 nm, and 144 nm, respectively. A narrow particle size distribution was obtained for all samples. Fig. 4 shows scanning electron micrographs for the nanoparticles produced by WSMM. The nanoparticles were partially covered by a film of the polymer (HPMC) after milling. A drop of the nanosuspension was placed on the silicon chip and dried overnight under vacuum. Rounded particles were observed for all the drugs as seen in Fig. 4. The morphology of the particles obtained after milling was similar for all three drugs.

3.2. Characterization of particles in film

3.2.1. SEM

SEM images for the surface of films are shown in Fig. 5. Although this mode is very qualitative, the visual observation provides an indication of particle dispersion. All images shown represent typical cases selected from many observations. Well-dispersed GF nanoparticles are observed in the film (Fig. 5a). Fig. 5b shows that some aggregation of particles is observed in FNB films (see arrow). The greatest aggregation of particles in film is observed for the NPX (Fig. 5c). At higher magnification (Fig. 5d) clusters of nanoparticles embedded in polymer can be seen. The aggregation of particles

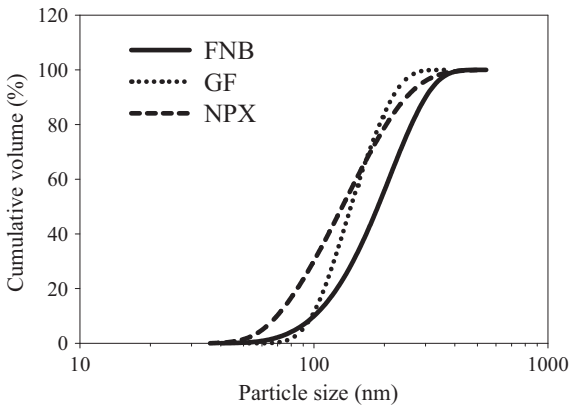

Fig. 3. Cumulative particle size distribution of the drug nanosuspensions after WSMM.

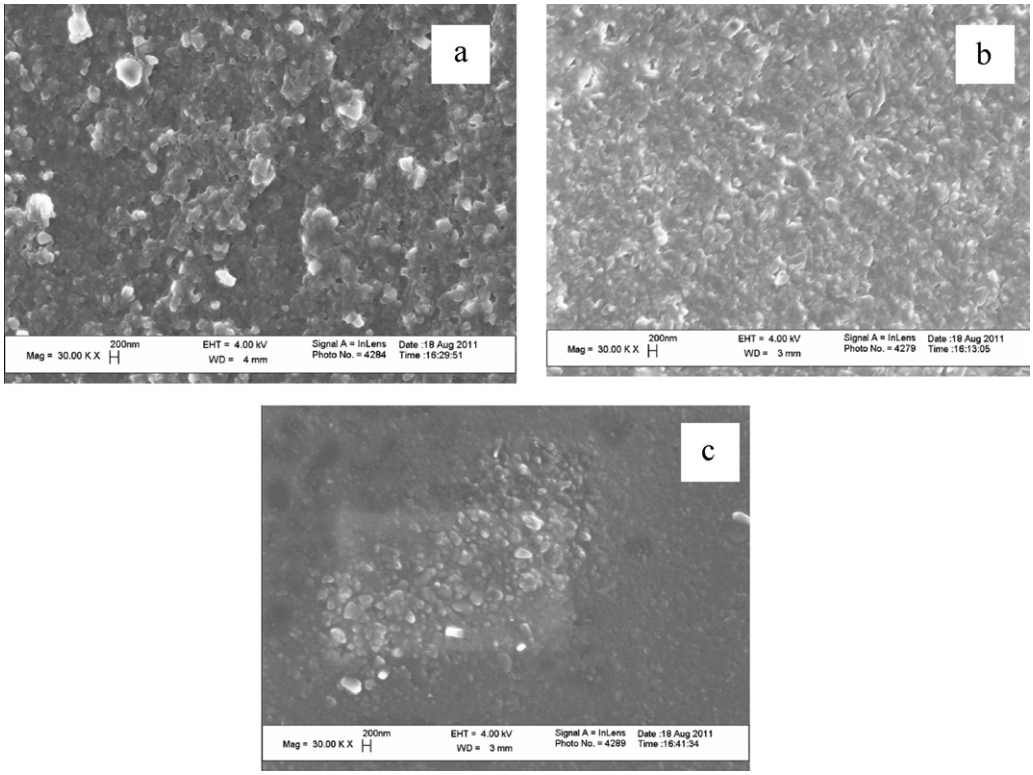

Fig. 4. SEM images of drug nanoparticles produced from WSMM. Shown are (a) GF, (b) FNB and (c) NPX. A drop of the nanosuspension was placed on the silicon chip and dried overnight under vacuum.

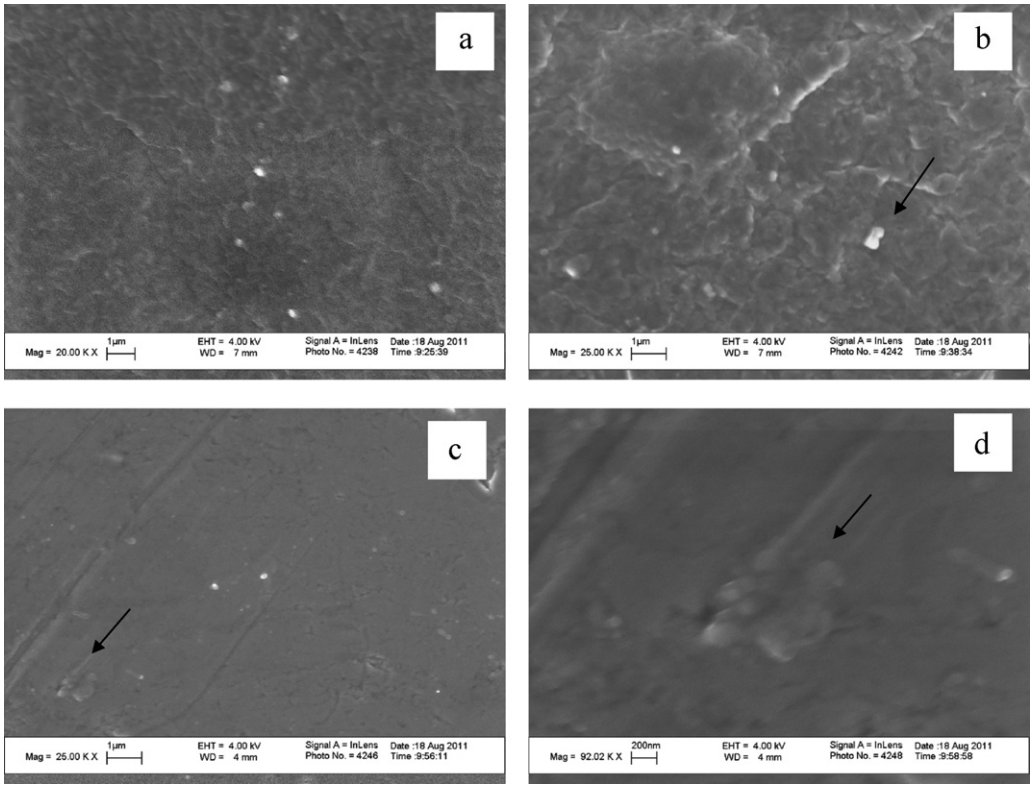

Fig. 5. SEM images of the surface of HPMC films containing dispersed drug nanoparticles. Shown are (a) GF, (b) FNB, (c) NPX, (d) NPX at a higher magnification. Arrows show aggregation of particles in film.

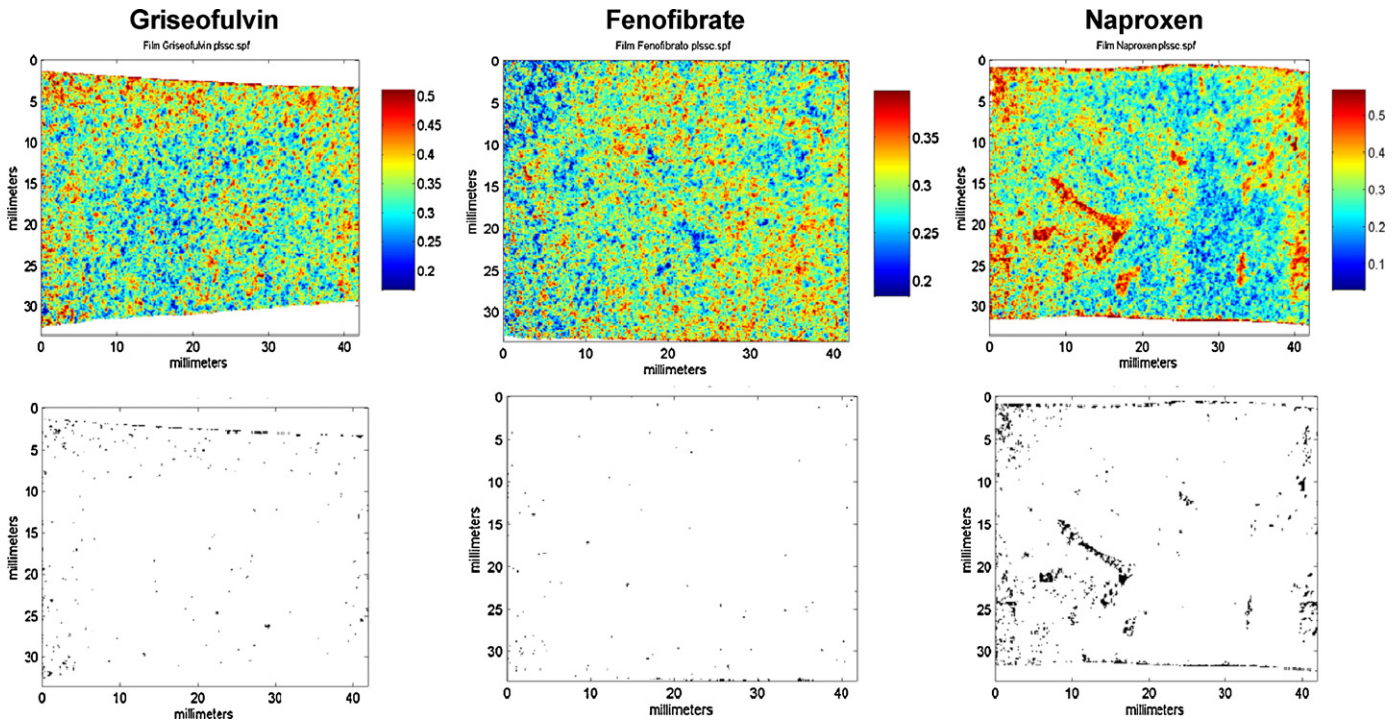

Fig. 6. NIR chemical images for films containing drug nanoparticles. (For interpretation of the references to color in the text, the reader is referred to the web version of the article.)

might have occurred during casting or film drying as the median particles size and particle size distributions do not change after mixing (178 nm for GF, 148 nm for NPX, and 219 nm for FNB). This behavior could be attributed to the strong hydrogen bonding of the carboxylic group in NPX (Nair et al., 2001; Hirasawa et al., 1998) as the water is removed and the drug concentration increased during drying. Further studies would be required to confirm these interactions

3.2.2. NIR chemical imaging

The aggregation behavior of nanoparticles in films was also evaluated using NIR chemical imaging. The NIR chemical imaging method complements the SEM analyses by evaluating drug distribution through a much larger film area, and is more quantitative in nature. Fig. 6 shows the distribution of NPX, GF and FNB throughout the surface of the films using the 131 μm/pixel objective. The score value scale is an indication of the spatial distribution and relative abundance of the drug. Abundance refers to drug distribution at a particular sampling point (film area analyzed by a pixel from the NIR chemical imaging system (de Juan et al., 2011). The top of the scale (red color in the color bar) indicates the highest contribution of drug to any pixel. Pixels rich in drug are observed in each of the analyzed areas. Areas of pure drug would be evidenced by an abundance value of 1.0 or 100%. The maximum score observed is about 0.6 in the NPX film. The mean value of the scores of drug in the entire set of pixels provides the bulk abundance (an estimate of the drug concentration in the bulk) (Lewis et al., 2005). The mean value obtained was 0.34 for GF, 0.29 for FNB, and 0.30 for NPX, as shown in Table 2. The mean values of the bulk abundance are all very close to the targeted 27% (w/w) film composition. Table 2 also reveals differences in the standard deviation of the score values. NPX had the highest standard deviation in the score values, and thus the greatest variation in drug distribution throughout the film. The FNB film has the mean value closest to the nominal value as indicated in Table 2, and the lowest standard deviation. Additionally, this film shows the lowest difference between the mean value and the minimum and maximum value observed in the PLS-DA classification scores. These results indicate that this film has the best drug distribution through the analyzed surface in comparison with the other two films analyzed.

Fig. 6 also shows binary images generated with the pixels of highest abundance of drug, as a way to facilitate the visualization of areas rich in drug and estimate the size of these areas. The pixels with scores that exceeded the mean value + 2 standard deviations were given a value of 1 (dark), and all others a value of zero. A visual examination of these images shows that the NPX film has a high drug content in certain localized areas. This film also presents the largest standard deviation for the score values and has the largest domain found in the three films. Films that have GF and FNB as active ingredients show better distribution of pixels rich in drug.

3.2.3. Drug crystallinity

XRD analysis was performed to study the crystal structure of drug in the film. Fig. 7 shows the spectra for GF, NPX, and FNB compared when these drugs are incorporated into HPMC films. The spectra obtained demonstrate that the drug in film has crystalline characteristics that are preserved during processing. To further corroborate these results Raman spectroscopy was employed. Fig. 8 shows the Raman spectra for the different pure drugs and drugs incorporated in film confirming crystallinity after film processing within the detection limits of the instrumentation. In GF, the lines at 560 and 640 cm^{-1} became two broadened peaks in the amorphous

Table 2
Distribution of drug nanoparticle in thin films according to drug score image using NIR-CI with a 131 μm/pixel objective.

	GF	FNB	NPX
Mean abundance API (%)	34	29.3	30
Standard deviations (%)	0.057	0.035	0.088
Minimum value (%)	20	20	10
Maximum value (%)	50	35	50
Lowest domain (mm^2)	0.02	0.03	0.02
Largest domain (mm^2)	0.65	0.50	2.49

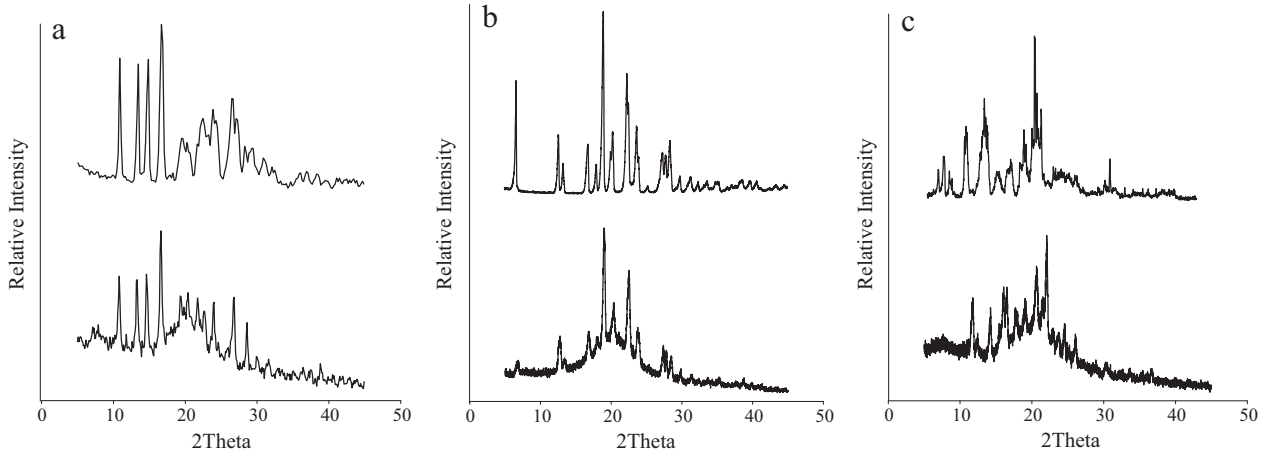

Fig. 7. X-ray diffractograms for drug (top) and film (bottom). Shown are (a) GF, (b) NPX, and (c) FNB.

phase, and the line at 822 cm^{-1}, attributed to cyclohexanone ring stretching vibrations disappeared with the decrease in crystallinity of the sample (Socrates, 2000; Żarów et al., 2011). This was not observed in the film in Fig. 5b indicating the presence of crystalline GF on film formation. Further studies will be required to corroborate crystal form and the presence of amorphous form as well. The broad Raman features near 1300 and 1800 cm^{-1} were due to the amorphous polymer gel substrate of the films.

3.3. Mechanical properties of films

Table 3 shows the Young's Modulus (YM), tensile strength (TS), elongation at break (*E*) and rupture force (RF) for the different films. Films have to be strong enough and ductile to prevent rupture of the dosage form during the cutting and packaging processes. A film that is too rigid (high YM) could also have an unpleasant sensation in the buccal cavity. The mechanical properties of polymer films are dependent on the polymer used and type and amount of plasticizer and surfactant (Cilurzo et al., 2008). Since the same formulation was used for GF and NPX the effect of drug type on the film mechanical properties can be studied by comparing these two samples. The type of drug used appears to have a prominent effect on the mechanical properties. The NPX films seem to be stronger than GF films as an increase of approximately 200% in YM is observed. This behavior could be due to a stronger interaction of NPX with the HPMC in the film compared to GF. Nair et al. (2001) has shown that NPX exhibit a stronger interaction with polyvinylpyrrolidone (PVP) films compared to GF. Similar behavior

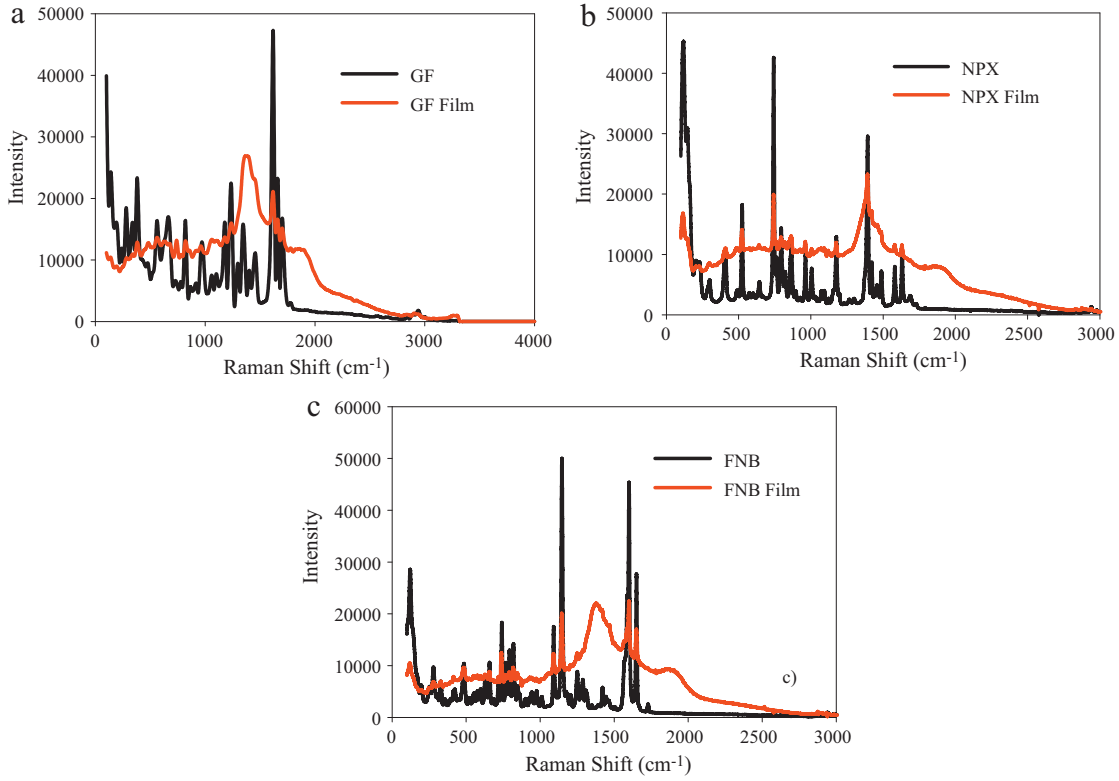

Fig. 8. Raman spectra for pure drug (black) and film (red) components and films. Shown are (a) GF, (b) NPX, and (c) FNB. (For interpretation of the references to color in the figure caption, the reader is referred to the web version of the article.)

Table 3
Mechanical properties for the different films loaded with drug nanoparticles (about 30% drug loading).

Sample	Young's Modulus (kPa) (average ± SD)	Tensile strength (kPa) (average ± SD)	Elongation at break (%) (average ± SD)	Rupture force (*N*) (average ± SD)
GF film	27.66 ± 5.50	157.92 ± 25.33	26.18 ± 6.24	0.32 ± 0.71
NPX film	82.50 ± 36.06	201.67 ± 41.33	11.23 ± 0.70	0.47 ± 0.75
FNB film	213.50 ± 27.57	644.70 ± 58.41	18.72 ± 0.31	1.04 ± 0.14

was confirmed for these films by using Fourier Transform Infrared (FTIR) Spectroscopy (results not shown). NPX exhibited a band at the 1730 cm^{-1} attributed to the carboxylic group that was shifted to higher infrared band indicating strong hydrogen bonding interaction in the film. On the other hand GF exhibited no change in band position indicating low or no interaction with the film. Similarly, TS and RF for NPX films were approximately 27% and 46% higher, respectively, compared to GF films although the difference is not statistically significant (p value < 0.05). The % elongation at break for NPX films was lower than GF films (133%) as expected.

In the case of FNB films, a lower amount of SDS was used to stabilize the suspensions during WSMM compared to NPX or GF and therefore differences in film properties could be observed (Rhim et al., 2002; Rodríguez et al., 2006). In fact, FNB exhibited approximately 650%, 300% and 225% increase in YM, TS, and RF, respectively compared to GF films. The increase in YM, TS and RF could be due to the lower SDS concentration in the film that decreases the molecular mobility related to the interaction of SDS with the polymer. Similar behavior has been observed for potato starch and whey protein isolate films containing SDS (Rhim et al., 2002; Rodríguez et al., 2006). Interestingly, the concentration of SDS in FNB in suspension is approximately 0.19% lower than the concentration of SDS in GF films. Therefore, this behavior could be attributed to a synergistic effect due to surfactant–polymer interaction and drug–polymer interaction as already presented for NPX films. More studies would be required to confirm these interactions. An increase in mechanical properties such as TS and RF will produce a film that is less prone to break (either by a tensile force or compressive force, respectively), more durable and easy to handle compared to a more fragile film.

3.4. Drug content

Fig. 9 shows the average content of drug per area for different batches with different thicknesses. As expected, increasing the thickness increases linearly the amount of drug. Therefore, thickness could be used to control dose in film dosage forms. GF films had a better linear fit with a r^2 value of 1.000 followed by FNB and NPX films with values of 0.958 and 0.901, respectively. The inferior linear fit of NPX is attributed to the aggregation of particles in films and relatively poor mixing/dispersion during the incorporation of the NPX nanosuspension into the viscous HPMC/glycerin solution, as confirmed by SEM and NIR chemical imaging.

As mentioned before, the theoretical amount of drug in the resulting film accounted for 27% (w/w) of the film composition, which is significant for a nanoparticle solid dosage form. As a reference, Tricor® formulations containing fenofibrate nanoparticles have a drug loading of approximately 22% (Ryde et al., 2007). We have been able to incorporate a higher amount of drug nanoparticles in a solid dosage form. Also, drug loading as high as 50% can be easily achieved by integrating WSMM and polymer films. Films with a thickness of 100 μm contain 4.5 mg FNB/cm^2. A film with the size of a postal stamp (6 cm^2) contains 27 mg FNB and could

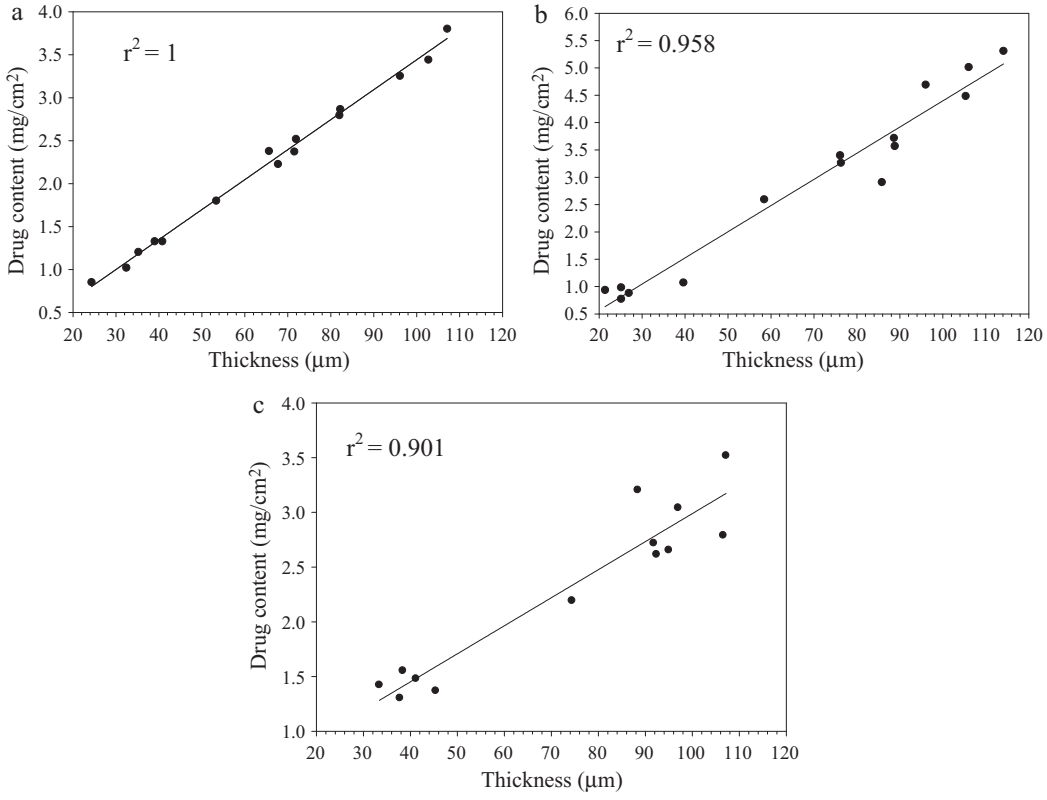

Fig. 9. Drug content for films with different thickness containing (a) GF, (b) FNB and (c) NPX nanoparticles.

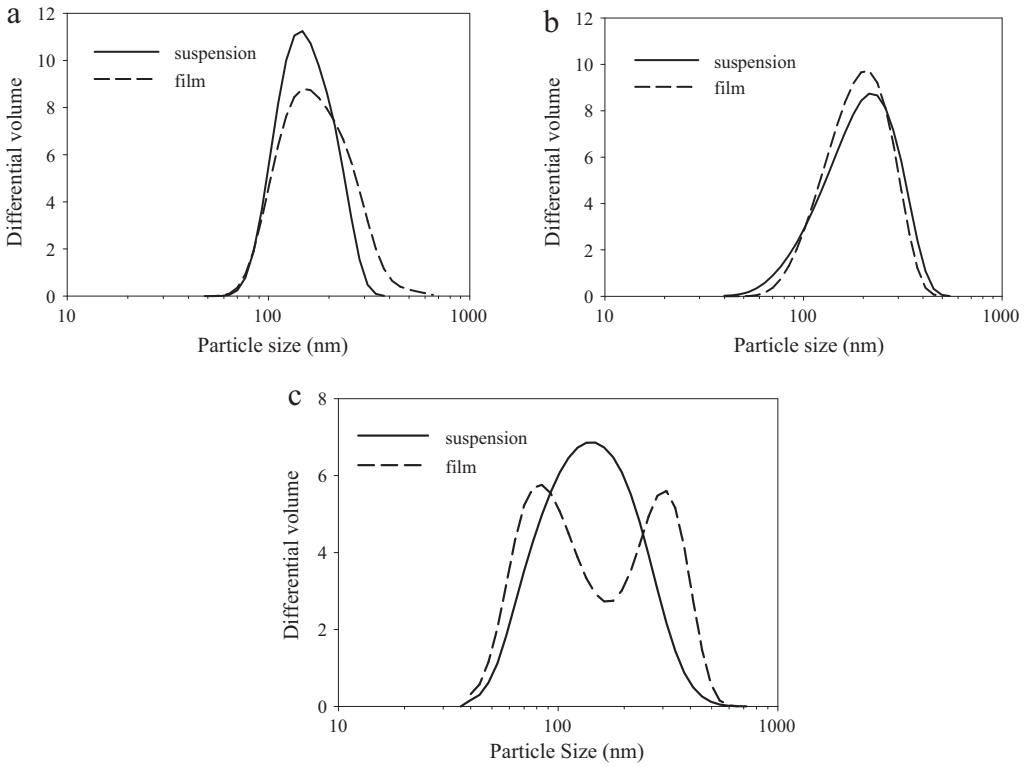

Fig. 10. Drug nanoparticles re-dispersion from films. Shown are (a) GF, (b) FNB and (c) NPX.

potentially contain 50 mg FNB with a higher loading. Higher doses could also be achieved by increasing the film thickness.

3.5. Re-dispersion of particles from films

Fig. 10 shows the particle size distribution for the nanosuspensions produced from WSMM and particle size distribution after re-dispersion from films for the different drugs. The median particle size of GF after re-dispersion was 175 nm compared to a median particle size of 163 nm for the suspension. Similarly the median particle sizes for FNB and NPX after re-dispersion were 256 nm and 145 nm, respectively compared to particles sizes of 207 nm and 144 nm, respectively. A bimodal distribution was observed for NPX particles after re-dispersion suggesting some aggregation of particles probably due to the strong secondary attraction of NPX particles. Nevertheless, all the drugs exhibited nanometer size scale dimensions after re-dispersion from films with sizes similar to the particles from nanosuspensions.

3.6. Dissolution

In order to prove the advantages of films over other solid dosage forms, the dissolution behavior of films containing FNB nanoparticles and films containing FNB microparticles were compared to a compact and a physical mixture of a similar composition as shown in Fig. 11a. The films exhibited a much faster dissolution rate compared to the other dosage forms. The rapid drug release of FNB from films was attributed to the high surface area available for wetting of the HPMC film. The films containing microparticles and nanoparticles exhibited a similar dissolution profile with ~20 min to reach the equilibrium dissolution. This behavior could be due to the high quantity of SDS in solution that makes the dissolution media non-discriminating. The time to dissolve 80% of the equilibrium concentration for the films is approximately 16 min. This result compares favorably with FNB formulations presented in patents

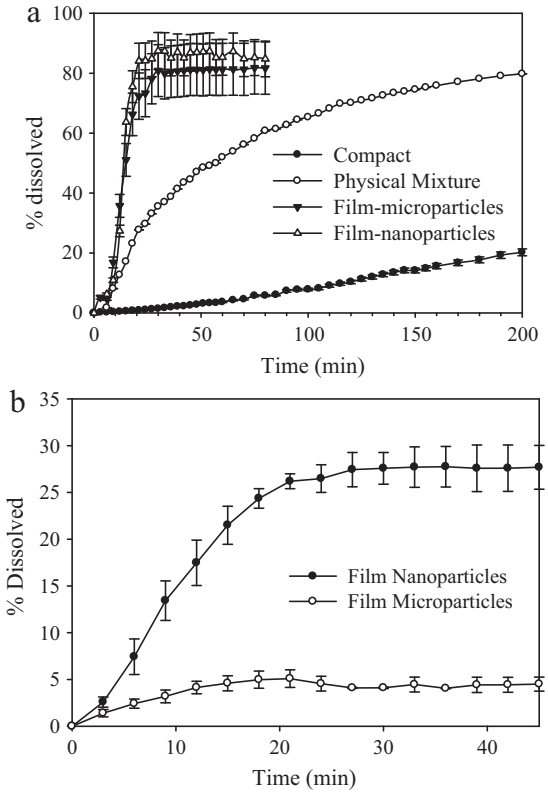

Fig. 11. Dissolution behavior (mean ± standard deviation, $n = 6$) of (a) FNB microparticles and nanoparticles in film compared to a physical mixture and a compact of the same physical mixture containing microparticles, and (b) films containing microparticles compared to film containing nanoparticles.

(Stamm and Seth, 2001) and commercially available formulations such as Tricor®, which take approximately 12–15 min to reach 80% of the equilibrium concentration (Jamzad and Fassihi, 2006, Sandal et al., 2011). As a point of reference, Tricor® formulation contains larger amount of SDS (1.5%) as compared to film formulation containing only 0.03%. Accordingly, although the film formulation has not been optimized with respect to fast disintegration and dissolution in the current work, films containing FNB nanoparticles exhibit similar dissolution behavior. The physical mixture took approximately 200 min to reach the same % dissolved. However, only 20% FNB dissolved from the compacts in 200 min. Although the film containing FNB nanoparticles as well as microparticles exhibited almost similar behavior, there are a few minor differences; films with nanoparticles exhibit a slight increase in % dissolved compared to the film containing microparticles, and the standard deviation for the nanoparticle films is less.

In order to further discriminate the dissolution behavior of films containing microparticles and nanoparticles, 100 ml of 0.025 M HCl was selected for dissolution studies to slow the dissolution rate and extent, and also allow for greater discrimination of particle size. Moreover, for good in vitro–in vivo correlations it is a common practice to use buffer solutions not exceeding pH 6.8 as the dissolution medium (Emami, 2006). 0.025 M HCl solution had a pH of 1.9 which simulates the pH of gastric fluid. A 0.2 μm filter (Pall HT Tuffryn Membrane Disc Filters) was used for this study. The previous dissolution medium containing SDS had a large amount of SDS (5.4%, w/w) above its CMC which led to the faster dissolution of both nano and microparticles of FNB. To confirm that the differences in dissolution are not due interference of presence of particles, samples after 10 min and at equilibrium were also filtered using a 0.1 μm syringe filter. No difference in absorbance was seen before and after filtering using UV spectrophotometry. The dissolution rate and extent of dissolution increased substantially for the films containing FNB nanoparticles (201 nm) compared to the film containing FNB microparticles (11 μm) as shown in Fig. 11b. FNB is a non-ionic drug and therefore it has a low solubility in the acidic medium which can explain the slow dissolution rate in comparison to the SDS buffer. However, this dissolution medium can clearly differentiate between the microparticles and nanoparticles of FNB as seen in Fig. 11b. Only about 5% dissolved for the films containing FNB microparticles compared to approximately 27% dissolved for the film containing FNB nanoparticles. A slight decrease in % dissolved was observed after reaching a maximum could be due to recrystallization of FNB in the medium. The increase in % dissolved by approximately a factor of 6 is probably due to the increased surface area of the drug and possible better contact between the nanoparticles and dissolution medium. Therefore, it appears that incorporation of nanoparticles into film formulations has a positive effect on the dissolution rate and extent, and potentially on bioavailability.

4. Summary and conclusions

In this study, the integration of nanosuspensions produced from wet stirred media milling (WSMM) into hydroxypropyl methyl cellulose (HPMC), which is bio-compatible and water-soluble polymer, films was demonstrated, providing a new route of transforming nanosuspensions of poorly water soluble, BCS Class II drugs into a solid dosage form. The simple process involved the casting and drying of a previously mixed stable drug nanosuspensions and polymer solution. Through this process, different drug nanoparticles were incorporated into HPMC films and their aggregation behavior in films was studied. Processing did not change the crystallinity of the drug particles. The results showed that the aggregation behavior is dependent on the drug used, and follows the trend: GF ≤ FNB ≤ NPX. The aggregation could be due to strong hydrophobic interactions of drug particles. The difference in aggregation also has a strong effect on the drug content in films. The strong hydrogen bonding interactions between the NPX and the HPMC allows also for improved film physical properties such as, increased Young's Modulus, Tensile Strength and Rupture Force compared to the GF films. This would allow for better handling during the cutting and packaging processes, although films that are too rigid could cause an unpleasant sensation in the patient's buccal cavity. The FNB films, which have a lower concentration of SDS due to stabilization requirements of the nanosuspension, exhibit an even higher increase in these properties due to a decrease in molecular mobility and also due to synergistic effect of surfactant-polymer interaction and drug–polymer interaction. The resulting film exhibits much faster dissolution rates compared to a physical mixture, a compact of similar formulation (having same surface area exposed to the dissolution medium) and a film containing microparticles. The films dissolved fast, thus allowing fast recovery and redispersion of the drug nanoparticles. Thus, polymer films are found to be an effective carrier of nanoparticles that were produced by media milling of BCS Class II drugs. High drug nanoparticles loading (as high as 50%) can also be easily obtained. The drug loading achieved is higher than current products in the market containing drug nanoparticles and the amount of drug in the film could be increased by increasing the film thickness. These results set the foundation for process development of films containing nanoparticles, specifically, for poorly water-soluble drugs, for various drug delivery applications. As compared to various routes to making solid dosage forms from drug nanosuspensions such as freeze drying, lyophilization, and spray drying, film formation may offer a more economical and scalable option. Future studies will focus on the effect of film formulation on particle re-dispersibility, drying effects on film mechanical properties, mixing characterization, stability and content uniformity of films.

Acknowledgements

The authors thank NSF for financial support of this project through the ERC (EEC-0540855) award. The authors also thank Golshid Keyvan for assistance with HPLC, Christian Beck for assistance with XRD, and Catharina Knieke for providing the FNB microparticles.

References

Amidon, G.L., Lennernäs, H., Shah, V.P., Crison, J.R., 1995. A theoretical basis for a biopharmaceutical drug classification: the correlation of in vitro drug product dissolution and in vivo bioavailability. Pharm. Res. 12, 413–420.

Bess, W.S., Kulkarni, N., Ambike, S.H., Ramsay, M.P., 2010. Fast dissolving orally consumable films containing a taste masking agent. US Patent 7,648,712.

Bhakay, A., Merwade, M., Bilgili, E., Dave, R.N., 2011. Novel aspects of wet milling for the production of microsuspensions and nanosuspensions of poorly water-soluble drugs. Drug Dev. Ind. Pharm. 37, 963–976.

Bhakay, A., Bilgili, E., Davé, R. Recovery of BCS Class II drug nanoparticles from core–shell type nanocomposite particles produced via fluidized bed coating. Powder Technology, under review.

Bilgili, E., Hamey, R., Scarlett, B., 2004. Production of pigment nanoparticles using a wet stirred media mill with polymeric media. China Particuol. 2, 93–100.

Bilgili, E., Hamey, R., Scarlett, B., 2006. Nano-milling of pigment agglomerates using a wet stirred media mill: elucidation of the kinetics and breakage mechanisms. Chem. Eng. Sci. 61, 149–157.

Boateng, J.S., Auffret, A.D., Matthews, K.H., Humphrey, M.J., Stevens, H.N.E., Gillian, M., 2010. Characterization of freeze-dried wafers and solvent evaporated films as potential drug delivery systems to mucosal surfaces. Int. J. Pharm. 389, 24–31.

Chan, K., Kazarian, S., 2004. Visualization of the heterogeneous water sorption in a pharmaceutical formulation under controlled humidity via FT-IR imaging. Vib. Spectrosc. 35, 45–49.

Cheow, W., Ng, M., Kho, K., Hadinoto, K., 2011. Spray-freeze-drying production of thermally sensitive polymeric nanoparticle aggregates for inhaled drug delivery: effect of freeze drying adjuvants. Int. J. Pharm. 404, 289–300.

Choi, J., Park, C., Lee, J., 2008. Effect of polymer molecular weight on nanocomminution of poorly soluble drug. Drug Deliv. 15, 347–353.

Choi, J.-Y., Yoo, J.Y., Kwak, H.-S., Nam, B.U., Lee, J., 2005. Role of polymeric stabilizers for drug nanocrystal dispersions. Curr. Appl. Phys., 472–474.
Cilurzo, F., Cupone, I.E., Minghetti, P., Selmin, F., Montanari, L., 2008. Fast dissolving films made of maltodextrins. Eur. J. Pharm. Biopharm. 70, 895–900.
de Juan, A., Tauler, R., Dyson, R., Marcolli, C., Rault, M., Maeder, M., 2011. Trends Anal. Chem. 23, 70–79.
Desieno, M.A., Stetsko, G., 1996. Redispersible nanoparticulate film matrices with protective overcoats. US Patent 5,573,783.
Dixit, R.P., Puthli, S.P., 2009. Oral strip technology: overview and future potential. J. Control. Release 139, 94–107.
El-Setouhy, D.A., Abd El-Malak, N.S., 2010. Formulation of a novel tianeptine sodium orodispersible film. AAPS Pharm. Sci. Tech. 11, 1018–1025.
Emami, J., 2006. In vitro–in vivo correlation: from theory to applications. J. Pharm. Pharmaceut. Sci. 9, 31–51.
Eskin, D., Zhupanska, O., Hamey, R., Moudgil, B., Scarlett, B., 2005. Microhydrodynamics of stirred media milling. Powder Technol. 156, 95–102.
Gao, L., Zhang, D., Chen, M., 2008. Drug nanocrystals for the formulation of poorly soluble drugs and its application as a potential drug delivery system. J. Nanopart. Res. 10, 845–846.
Garsuch, V., Breitkreutz, J., 2010. Comparative investigations on different polymers for the preparation of fast-dissolving oral films. J. Pharm. Pharmacol. 62, 539–545.
Hanafy, A., Spahn-Langguth, H., Vergnault, G., Grenier, P., Tubic Grozdanis, M., Lenhardt, T., Langguth, P., 2007. Pharmacokinetic evaluation of oral fenofibrate nanosuspensions and SLN in comparison to conventional suspensions of micronized drug. Adv. Drug Deliv. Rev. 59, 419–426.
Heng, D., Cutler, D.J., Chan, H.-K., Yun, J., Raper, J.A., 2008. What is a suitable dissolution method for drug nanoparticles. Pharm. Res. 25, 1696–1701.
Heng, D., Ogawa, K., Cutler, D.J., Chan, H., Raper, J.A., Ye, L., Yun, J., 2010. Pure drug nanoparticles in tablets: what are the dissolution limitations? J. Nanopart. Res. 12, 1743–1754.
Hernandez-Trejo, N., Kayser, O., Steckel, H., Müller, R.H., 2005. Characterization of nebulized buparvaquone nanosuspensions-effect of nebulization technology. J. Drug Target 13, 499–507.
Hirasawa, N., Danjo, K., Haruna, M., Otsuka, A., 1998. Physicochemical characterization and drug release studies of naproxen solid dispersions using lactose as a carrier. Chem. Pharm. Bull. 46, 1027–1030.
Hu, J., Ng, W., Dong, Y., Shen, S., Tan, R., 2011. Continuous and scalable process for water redispersible nanoformulation of poorly aqueous soluble APIs by antisolvent precipitation and spray drying. Int. J. Pharm. 404, 198–204.
Jamzad, S., Fassihi, R., 2006. Role of surfactant and pH on dissolution properties of fenofibrate and glipizide—a technical note. AAPS Pharm. Sci. Tech. 7 (article 33) http://www.aapspharmscitech.org.
Jérez Rozo, J.I., Zarow, A., Zhou, B., Pinal, R., Iqbal, Z., Romañach, R.J., 2011. Complementary near-infrared and Raman chemical imaging of pharmaceutical thin films. J. Pharm. Sci., doi:10.1002/jps.22653, Published online in Wiley Online Library http://www.wileyonlinelibrary.com.
Jug, M., Bećirević-Laćan, M., Bengez, S., 2009. Novel cyclodextrin-based film formulation intended for buccal delivery of atenolol. Drug Dev. Ind. Pharm. 35, 796–807.
Kakhi, M., 2009. Classification of the flow regimes in the flow-through cell. Eur. J. Pharm. Biopharm. 37, 531–544.
Keck, C.M., Muller, R.H., 2006. Drug nanocrystals of poorly soluble drugs produced by high pressure homogenization. Eur. J. Pharm. Biopharm. 62, 3–16.
Kesisoglou, F., Panmai, S., Wu, Y., 2007. Nanosizing-oral formulation development and biopharmaceutical evaluation. Adv. Drug Deliv. Rev. 59, 631–644.
Kim, S., Lee, J., 2010. Effective polymeric dispersants for vacuum, convection and freeze drying of drug nanosuspensions. Int. J. Pharm. 397, 218–224.
Krishnaiah, Y.S.R., 2010. Pharmaceutical technologies for enhancing oral bioavailability of poorly soluble drugs. J. Bioequiv. Bioavail. 2, 28–36.
Lee, J., 2003. Drug nano- and microparticles processed into solid dosage forms: physical properties. J. Pharm. Sci. 92, 2057–2068.
Lee, J., Cheng, Y., 2006. Critical freezing rate in freeze drying nanocrystal dispersions. J. Control. Release 111, 185–192.
Lewis, E.N., Schoppelrei, J.W., Lee, E., Kidder, L.H., 2005. Near-infrared chemical imaging as a process analytical tool. In: Katherine, A.B. (Ed.), Chapter 7 in Process Analytical Technology. Blackwell Publishing, Oxford, UK, pp. 187–225.
Li, H., Gu, X., 2007. Correlation between drug dissolution and polymer hydration: a study using texture analysis. Int. J. Pharm. 342, 18–25.
Liversidge, G., Cundy, K., 1995. Particle size reduction for the improvement of oral bioavailability of hydrophobic drugs: I. Absolute oral bioavailability of nanocrystalline danazol in Beagle dogs. Int. J. Pharm. 125, 91–97.
Matthews, K.H., Stevens, H.N.E., Auffret, A.D., Humphrey, M.J., Eccleston, G.M., 2008. Formulation, stability and thermal analysis of lyophilised wound healing wafers containing an insoluble MMP-3 inhibitor and a non-ionic surfactant. Int. J. Pharm. 356, 110–120.
Mauludin, R., Müller, R.H., Keck, C.M., 2009. Development of an oral rutin nanocrystal formulation. Int. J. Pharm. 370, 202–209.
Mende, S., Stenger, F., Peukert, W., Schwedes, J., 2003. Mechanical production and stabilization of submicron particles in stirred media mills. Powder Technol. 132, 64–73.
Mendoza-Romeroa, L., Piñón-Segundo, E., Nava-Arzaluz, M., Ganem-Quintanar, A., Cordero-Sánchez, S., Quintanar-Guerrero, D., 2009. Comparison of pharmaceutical films prepared from aqueous polymeric dispersions using the cast method and the spraying technique. Colloids Surf. A: Physicochem. Eng. Aspects 337, 109–116.
Merisko-Liversidge, E., Liversidge, G.G., 2011. Nanosizing for oral and parenteral drug delivery: a perspective on formulating poorly-water soluble compounds using wet media milling technology. Adv. Drug Deliv. Rev. 63, 427–440.
Merisko-Liversidge, E., Liversidge, G.G., Cooper, E.R., 2003. Nanosizing: a formulation approach for poorly-water-soluble compounds. Eur. J. Pharm. Sci. 18, 113–120.
Müller, R.H., Möschwitzer, J., Bushrab, F.N., 2006. Manufacturing of nanoparticles by milling and homogenization techniques. In: Gupta, R.B., Kompella, U.B. (Eds.), Nanoparticle Technology for Drug Delivery, Drugs and the Pharmaceutical Sciences, vol. 159. Taylor & Francis Group, LLC, New York, pp. 21–51.
Muller, R.H., 2011. Nanosuspensions as particulate drug formulations in therapy: rationale for development and what we can expect in the future. Adv. Drug Deliv. Rev. 47, 3–19.
Nair, R., Nyamweya, N., Gönen, S., Martínez-Miranda, L.J., Hoag, S.W., 2001. Influence of various drugs on the glass transition temperature of poly(vinylpyrrolidone): a thermodynamic and spectroscopic investigation. Int. J. Pharm. 225, 83–96.
Nishimura, M., Matsuura, K., Tsukioka, T., Yamashita, H., Inagaki, N., Sugiyama, T., Itoh, T., 2009. In vitro and in vivo characteristics of prochlorperazine oral disintegrating film. Int. J. Pharm. 368, 98–102.
Noyes, A.A., Whitney, W.R., 1897. The rate of solution of solid substances in their own solutions. J. Am. Chem. Soc. 19, 930–934.
Panagiotou, T., Fisher, R.J., 2008. Form nanoparticles via controlled crystallization. Chem. Eng. Prog., 33–39.
Pathak, P., Meziani, M.J., Sun, Y.-P., 2005. Supercritical fluid technology for enhanced drug delivery. Expert Opin. Drug Deliv. 2, 747–761.
Perumal, V.A., Lutchman, D., Mackraj, I., Govender, T., 2008. Formulation of monolayered films with drug and polymers of opposing solubilities. Int. J. Pharm. 358, 184–191.
Petersen, R., 2006. Nanocrystals for use in topical cosmetic formulations and method of production thereof. US Patent 8,866,233.
Peukert, W., Schwarzer, H., Stenger, F., 2005. Control of aggregation in production and handling of nanoparticles. Chem. Eng. Process 44, 245–252.
Piao, H., Kamiya, N., Hirata, A., Fujii, T., Goto, M.A., 2008. Novel solid-in-oil nanosuspension for transdermal delivery of diclofenac sodium. Pharm. Res. 25, 896–901.
Ploehn, H.J., Russel, W.B., 1990. Interactions between colloidal particles and soluble polymers. Adv. Chem. Eng. 15, 137–228.
Pu, X., Sun, J., Li, M., He, Z., 2009. Formulation of nanosuspensions as a new approach for the delivery of poorly soluble drugs. Curr. Nanosci. 5, 417–427.
Rabinow, B., Kipp, J., Papadopoulos, P., Wong, J., Glosson, J., Gass, J., Sun, C.S., Wielgos, T., White, R., Cook, C., Barker, K., Wood, L., 2007. Itraconazole IV nanosuspension enhances efficacy through altered pharmacokinetics in the rat. Int. J. Pharm. 339, 251–260.
Radebaugh, G.W., Murtha, J.L., Julian, T.N., Bondi, J.N., 1988. Methods for evaluating the puncture and shear properties of pharmaceutical polymeric films. Int. J. Pharm. 45, 39–46.
Rhim, J.W., Gennadios, A., Weller, C.L., Hanna, M.A., 2002. Sodium dodecyl sulfate treatment improves properties of cast films from soy protein isolate. Ind. Crop Prod. 15, 199–205.
Rodríguez, M., Osés, J., Ziani, K., Maté, J.I., 2006. Combined effect of plasticizers and surfactants on the physical properties of starch based edible films. Food Res. Int. 39, 840–846.
Ryde, T., Gustow, E., Ruddy, S.B., Jain, R., Wilkins, M.J., 2007. Nanoparticulate fibrate formulations. US Patent 7,276,249.
Ryde, T., Gustow, E., Ruddy, S.B., Jain, R., Wilkins, M.J., 2008. Methods of treatment using nanoparticulate fenofibrate compositions. US Patent 7,320,802.
Sandal, R., Thakkar, V., Gundu, R.K., Dabre, R.S., Murali, N., Jain, G.K., 2011. Pharmaceutical compositions comprising adsorbate of fenofibrate. US Patent US 2011/097414 A1.
Schmidt, C., Bodmeier, R., 1999. Incorporation of polymeric nanoparticles into solid dosage forms. J. Control. Release 57, 115–125.
Shegokar, R., Müller, R.H., 2010. Nanocrystals: industrially feasible multifunctional formulation technology for poorly soluble actives. Int. J. Pharm. 399, 129–139.
Shimoda, H., Taniguchi, K., 2009. Preparation of fast dissolving oral thin film containing dexamethasone: a possible application to antiemesis during cancer chemotherapy. Eur. J. Pharm. Biopharm. Biopharm. 73, 361–365.
Socrates, G., 2000. Infrared and Raman Characteristic Group Frequencies, 3rd ed. John Wiley & Sons, Ltd., England.
Stamm, A., Seth, P., 2001. Fenofibrate pharmaceutical composition having high bioavailability and method for preparing it. US Patent 6,277,405.
Timpe, C., 2010. Drug solubilization strategies applying nanoparticulate formulation and solid dispersion approaches, drug development. Pharm. Rev. 13, 12–21.
Van Eerdenbrugh, B., Van den Mooter, G., Augustijns, P., 2008a. Top-down production of drug nanocrystals: nanosuspension stabilization, miniaturization and transformation into solid products. Int. J. Pharm. 364, 64–75.
Van Eerdenbrugh, B., Vercruysse, S., Martens, J.A., Vermant, J., Froyen, L., Van Humbeeck, G., Van den Mooter, G., Augustijns, P., 2008b. Microcrystalline cellulose, a useful alternative for sucrose as a matrix former during freeze-drying of drug nanosuspensions—a case study with itraconazole. Eur. J. Pharm. Biopharm. 70, 590–596.
Van Eerdenbrugh, B., Froyen, L., Van Humbeeck, G., Martens, J.A., Augustijns, P., Van den Mooter, G., 2008c. Drying of crystalline drug nanosuspensions—the importance of surface hydrophobicity on dissolution behavior upon redispersion. Eur. J. Pharm. Biopharm. 35, 127–135.

Van Eerdenbrugh, B., Vermant, J., Martens, J.A., Froyen, L., Van Humbeeck, J., Augustijns, P., Van demMooter, G., 2009. A screening study of surface stabilization during the production of drug nanocrystals. J. Pharm. Sci. 98, 2091–2103.
Vergote, G.J., Nervaet, C., Van Driessche, I., Hoste, S., De Smedt, S., Demeester, J., Jain, R.A., Ruddy, S., Remon, J.P., 2001. An oral controlled release matrix pellet formulation containing nanocrystalline ketoprofen. Int. J. Pharm. 219, 81–87.
Verma, S., Kumar, S., Gokhale, R., Burgess, D., 2011. Physical stability of nanosuspensions: investigation of the role of stabilizers on Ostwald ripening. Int. J. Pharm. 15, 145–152.
Yang, R.K., Fuisz, R.C., Myers, G.L., Fuisz, J.M., 2010. Method of making self-supporting therapeutic active-containing film. US Patent 7,824,588.
Yang, R.K., Fuisz, R.C., Myers, G.L., Fuisz, J.M., 2011. Process for forming an ingestible thin film with non-self-aggregating uniform heterogeneity. US Patent 7,910,031.
Żarów, A., Zhou, B., Wang, X., Pinal, R., Iqbal, Z., 2011. Spectroscopic and X-ray diffraction study of structural disorder in cryomilled and amorphous Griseofulvin. Appl. Spectrosc. 65, 135–143.